

EXPERIMENTAL STUDY OF THE  
SEPARATION AND REATTACHMENT IN  
A PARTIALLY CONFINED JET

Thesis by

James J. Kosmicki

In Partial Fulfillment of the Requirements  
for the Degree of  
Aeronautical Engineer

California Institute of Technology  
Pasadena, California  
1973

(Submitted March 23, 1973)

## ACKNOWLEDGMENTS

The author wishes to express his appreciation to Dr. Anatol Roshko for the advice and guidance received through the course of this work.

It is also with gratitude that he acknowledges the help of Mrs. Geraldine Krentler in the preparation of this script.

Finally thanks are due to the California Institute of Technology for the opportunity to study in the Institute and for the financial assistance received.

## ABSTRACT

By use of various lengths of shroud an experimental study was made of a partially confined jet to examine the transition between the flow configuration for a free jet to that of a confined jet. An examination of the reattachment pressure distributions and the parameters at the entrance of the abrupt channel expansion was made. A smooth transition of mean flow quantities was found to occur in the transition from a free jet to a partially confined jet and then to a fully confined jet. The distance to reattachment was measured for various shroud lengths and shown to exhibit an asymptotic value which was Reynolds number dependent. Associated with this maximum reattachment length was a maximum pressure recovery factor. The range of Reynolds numbers - based upon the jet diameter - for the present study was 80,000 to 280,000.

## TABLE OF CONTENTS

| PART | TITLE   | PAGE |
|------|---|------|
|      | Acknowledgments   | ii   |
|      | Abstract  | iii  |
|      | Table of Contents                                       | iv   |
|      | Nomenclature  | vi   |
|      | List of Figures   | viii |
| I.   | Introduction  | 1    |
| II.  | Description of Apparatus and Experimental<br>Techniques | 4    |
|      | Overview  | 4    |
|      | Wind Tunnel   | 5    |
|      | Shroud  | 5    |
|      | Traversing Mechanism                                    | 6    |
|      | Pressure Measurements                                   | 6    |
|      | Velocity Measurements                                   | 7    |
|      | Reattachment Location                                   | 7    |
|      | Test Matrix   | 9    |
| III. | Results and Discussion                                  | 10   |
|      | Reattachment Pressure Distribution                      | 10   |
|      | Radial Pressure Distribution                            | 12   |
|      | Mean Velocity   | 12   |
|      | Shroud Length Effects                                   | 13   |

## TABLE OF CONTENTS (cont.)

| PART | TITLE       | PAGE |
|------|-------------|------|
| IV   | Conclusions | 17   |
|      | References  | 18   |
|      | Figures     | 20   |

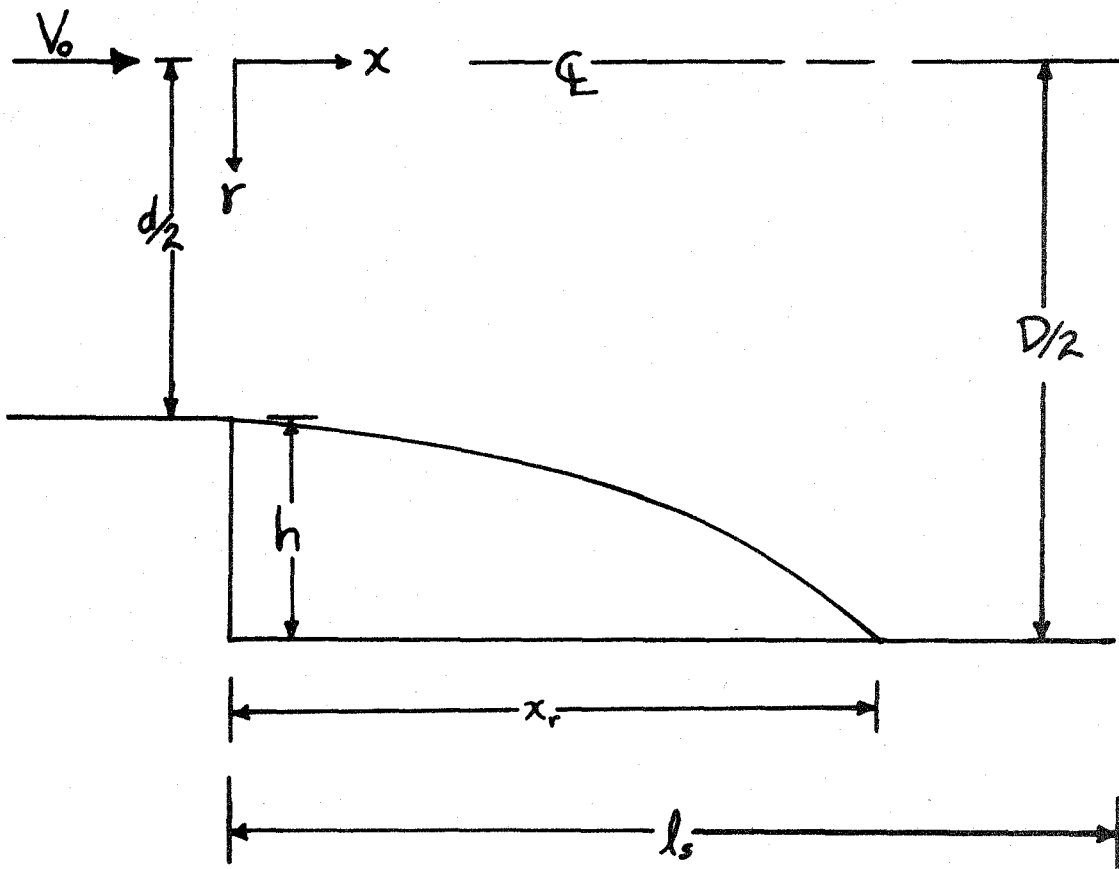
## NOMENCLATURE

|               |   |   |
|---------------|---|---|
| $C_p$         | = | pressure coefficient = $\frac{p - p_o}{\frac{1}{2} \rho V_o^2}$   |
| $\tilde{C}_p$ | = | reduced pressure coefficient = $\frac{p - p_1}{\frac{1}{2} \rho u_1^2} = \frac{C_p - C_{p1}}{1 - C_{p1}}$ |
| $\bar{C}_p$   | = | overall pressure recovery coefficient = $\frac{p_a - p_o}{\frac{1}{2} \rho V_o^2}$                        |
| D             | = | shroud diameter   |
| d             | = | nozzle diameter   |
| h             | = | step height   |
| $l_s$         | = | shroud length   |
| p             | = | pressure  |
| $p_e$         | = | pressure at shroud exit   |
| r             | = | radial distance measured from jet centerline  |
| Re            | = | Reynolds number - based upon $d/2$  |
| x             | = | streamwise distance measured from the step  |
| $x_r$         | = | reattachment length   |
| $\sigma$      | = | pressure recovery factor $\frac{C_p - C_{p1}}{1 - C_{p1}}$  |
| $\alpha$      | = | area ratio of the circular channel expansion  |

## Subscripts

|   |  |
|---|--|
| 1 | constant pressure portion of shear layer |
| 2 | maximum pressure location                |
| r | reattachment point                       |
| o | nozzle main flow conditions              |
| a | ambient condition                        |

## NOMENCLATURE



## LIST OF FIGURES

1. Sketch by Leonardo da Vinci.
2. General Patterns of Flow from Slot and Orifice.
3. General Pattern of the Flow of a Confined Jet.
4. Separation Bubble on an Aerofoil.
5. Test Section Configuration.
6. Schematic of the Experimental Setup.
7. Reattachment Pressure Distribution. ( $V_o = 24.8$  ft/sec)
8. Reattachment Pressure Distribution. ( $V_o = 54.8$  ft/sec)
9. Reattachment Pressure Distribution. ( $V_o = 83.4$  ft/sec)
10. Radial Pressure Distribution.
11. Mean Velocity Profiles and Streamline Patterns.
12. Overall Pressure Recovery Coefficient for Changing Shroud Lengths.
13. Change of Main Flow Velocity ( $V_o$ ) Due to Changes of Shroud Lengths.
14. Reattachment Lengths ( $x_r$ ).
15. Reattachment Pressure Recovery Coefficient ( $\sigma_r$ ).



## I. INTRODUCTION

As far back in history as the time of Leonardo da Vinci (Fig. 1) scientists and engineers have been interested in flow separation and downstream reattachment.

There are many problems in separated flow (Ref. 1), but one of the simplest is flow over a downstream facing step. For example, Moore (Refs. 2, 3) and Tani (Ref. 4) investigated the two dimensional problem by use of a rearward facing step on a wind tunnel wall. They varied both the step height and the main flow velocity and studied the wall pressure distribution downstream of the step. Chaturvedi (Ref. 5) and Back and Roschke (Ref. 6) used an abrupt circular channel expansion downstream of a jet nozzle (i. e. , a confined jet) to investigate the axisymmetric case.

All the above investigations had a sufficiently long channel downstream of the separation point to ensure reattachment.

A free jet itself is an example of flow separation with no subsequent reattachment (actually it may be considered to reattach at infinity corresponding to an infinite step height). This flow is also well documented.

A free jet is capable of entraining the necessary mass from its surroundings through the velocity induced by the shear layer (Fig. 2). On the other hand a confined jet cannot entrain the required mass from its surroundings, and must supply itself somehow. To do so a reverse flow pattern is established (Fig. 3). According to the findings of Seban, Emery, and Levy (Ref. 7) this pattern is a circulatory flow

which appears to be steady and which provides an upstream velocity of the order of  $1/5$  the free stream velocity. Macagno and Hung (Ref. 8) concluded that this eddy fills the role of helping to shape the mainflow in a streamline fashion while providing the required recirculating entrainment flow to the separated shear layer. These two cases, a free jet and a confined jet, are quite different. A free jet has no pressure gradient in the streamwise direction but entrains mass from its surroundings. A confined jet has large pressure gradients in the streamwise direction but entrains no mass from its surroundings. This raises the question - what are the characteristics of a partially confined jet?

To investigate this question and study the transition from one limiting case to the other, shrouds of various lengths were placed around a free jet. For very short shroud lengths the flow is that of a free jet, but for long shroud lengths the flow is that of a confined jet. At intermediate shroud lengths the jet is partially confined. As will be shown later, there is a smooth transition from the free jet to the confined jet flow configurations. Reattachment pressure distributions showed a smooth rise along the shroud joining a region of constant pressure just downstream of the step with a region of constant pressure a short distance downstream of the shroud exit in all cases, whether the separated flow had reattached to the shroud surface or remained unattached. Various reattachment parameters were investigated and a relation between the length of the reattachment bubble and the pressure recovery coefficient was found. An asymptotic reattachment length was determined and found to be Reynolds

number dependent whereas the maximum reattachment pressure recovery coefficient was found to be approximately equal to 0.34 for all three Reynolds numbers.

Owen and Klanfer (Ref. 9) established a criterion by which they could relate the length of the leading edge separation reattachment bubble on an aerofoil to a Reynolds number related to conditions at separation.

Norbury and Crabtree (Ref. 10) developed a simplified model giving particular attention to the reattachment process. In essence, they used the model shown in figure 4, making the assumption that the principal mixing and corresponding pressure recovery occurred in the region between points (1) and (2). They then proposed that the best correlation for the bubble reattachment region could be obtained in terms of a pressure recovery factor of the form

$$\sigma = \frac{p_2 - p_1}{\frac{1}{2} \rho V_1^2}$$

where  $p_1$  is the static pressure just downstream of separation,  $p_2$  is the maximum pressure downstream of reattachment, and  $V_1$  is the velocity just downstream of separation along the shear layer.

The pressure recovery coefficient,  $\sigma$ , can be written in terms of the normal pressure coefficient

$$\sigma = \frac{C_{p_2} - C_{p_1}}{1 - C_{p_1}}$$

In view of the assumptions made there exists a maximum value of  $\sigma$  for which reattachment must occur, but reattachment may occur for

values of  $\sigma$  less than this maximum.

Another useful, often used coefficient is the pressure recovery coefficient evaluated at the point where the dividing streamline closes on a solid surface. The reattachment pressure recovery factor,  $\sigma_r$ , was evaluated at the point of reattachment as

$$\sigma_r = \frac{C_{p_r} - C_{p_1}}{1 - C_p}$$

in the present study and is plotted for changing shroud length in figure 15.

## II. DESCRIPTION OF APPARATUS AND EXPERIMENTAL TECHNIQUES

### Overview

A low speed jet capable of velocities up to 92 ft/sec was used for the investigation. An axisymmetric channel expansion was achieved by placing shrouds of various lengths and constant diameter around the nozzle of the jet. Measurements of the mean velocity and pressure were made in both the streamwise and radial directions using a pitot-static tube mounted on a mechanical traversing mechanism. Reattachment point, defined as that point on the shroud where the difference between surface pitot and static pressures was zero, was located and a reattachment pressure recovery factor was evaluated at that point.

## Wind Tunnel

All tests were conducted on one of the six inch free jets located in the Fluid Mechanics Department of the Graduate Aeronautical Laboratories, California Institute of Technology. The jet assembly consisted of a variable speed fan driven by an electric motor, a honeycomb section to control turbulence, a settling chamber, and a contraction section that forms a six inch diameter jet nozzle (Fig. 6).

The rpm of the fan could be accurately regulated via a gear mechanism to achieve main flow velocities at the nozzle of 20 ft/sec to 92 ft/sec.

## Shroud

An aluminum shroud was used to achieve a one inch axisymmetric step. The shroud was fitted over the jet nozzle and held in place by two aluminum collars (Fig. 5). This gave the shroud a close fit at the step and kept the alignment parallel to the centerline to maintain axisymmetric flow. The shroud could be moved in the streamwise direction to provide continuous values of  $l_s/h$  from 0.0 to 18.0 ( $l/d = 0.0$  to 3.0).

Tani (Ref. 4) found that the streamwise wall pressure distribution is rather insensitive to changes in step height for the two dimensional case. In view of this a one inch step height was chosen and not changed during the investigation. This gave a ratio of step height to nozzle radius of 1/3 for which separation and reattachment could be considered to behave much as in the two dimensional case.

### Traversing Mechanism

The pitot-static tube was attached to a traversing mechanism for streamwise and radial traverses and positioning. The traversing mechanism was kept well below the flow of the jet. Measurements of position using the traversing system were read to 0.01 inches. Movement was accomplished by use of a hand-operated screw.

### Pressure Measurements

The dynamic and static pressures were measured on a Barocel electronic manometer system with readouts displayed on an integrating digital multimeter from which they were visually averaged and recorded. The Barocel manometer system had a manufacturer's specified error of less than .25% of the reading. Static pressures could be measured along the nozzle by pressure tappings at positions 2.0, 4.0 and 6.0 inches upstream of the step and 0.5 inches radially below the step shoulder at four angular positions spaced  $90^{\circ}$  apart around the circumference of the collar.

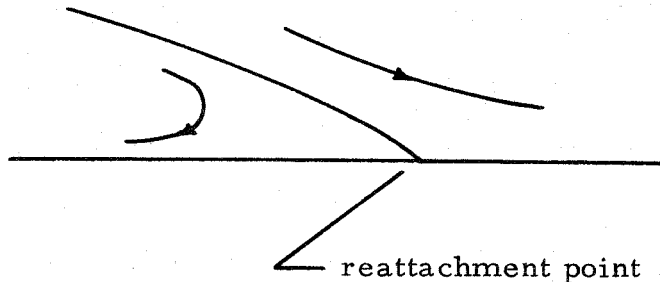
$p_o$ , the main flow static pressure, was measured on the nozzle wall 2.0 inches upstream of the step. The inside diameter of the pressure tappings was 0.020 inches. The proper orifice was connected to one leg of the manometer through a manual switching Scanivalve. The pitot-static and static tubes could be mounted on the traversing mechanism when needed and were used to measure dynamic and static pressures.

### Velocity Measurements

The main flow reference velocity,  $V_o$ , was determined by a pitot-static tube located on the centerline of the jet 2.0 inches upstream of the plane of the step. A pitot-static tube placed on the traversing mechanism was used to measure dynamic head to determine the velocity profile. Negative values of dynamic head simply indicated reverse flow and were not used to determine absolute magnitudes.

### Reattachment Location

The reattachment point is defined as the point of flow stagnation on the surface of the shroud.



Two approaches were used to locate the reattachment point. The first was to observe the surface flow direction by use of a thin oil film. A mixture of light machine oil and titanium dioxide was painted onto the surface of the shroud. In a small region where the flow was stagnant the powder particles were not moved; on either side the solution was carried away by the flow. The region of no movement was taken to be the reattachment region. The size of this reattachment region was of the order of 1/8 inch.

The second method was to record the pitot static pressure difference measured by a probe dragged along the shroud surface. The reattachment point was then defined as the point at which the difference was equal to zero. The second method was found to give a smaller degree of uncertainty since curves drawn through several static and several dynamic pressure readings along the shroud could be used to locate the zero point. Therefore the length determined by this method is taken to be the reattachment length plotted in figure 14 and was used in all subsequent calculations.

The reattachment point is indicated on the reattachment pressure distributions in figures 7, 8, and 9 by the solid symbols.



Test Matrix

Procedures used to obtain the data presented in the figures which accompany this work are shown below. (The step height,  $h$ , and the upstream diameter,  $d$ , were held constant through the investigation.)

| <u>Figures</u> | <u>Parameters held constant</u>      | <u>varied</u> | <u>Quantity Measured</u>                | <u>Objectives</u>                      |
|----------------|--------------------------------------|---------------|---|--|
| 7, 8, 9        | $V_o, r$                             | $x$           | $p - p_o$<br>$\frac{1}{2} \rho V_o^2$   | reattachment pressure distribution     |
| 10             | $V_o, l_s$                           | $r$           | $p - p_o$<br>$\frac{1}{2} \rho V_o^2$   | radial pressure distribution           |
| 11             | $V_o, l_s$                           | $r$           | $V_o$                                   | mean velocity profiles and streamlines |
| 12             | $V_o, x, r$                          | $l_s$         | $p_a - p_o$<br>$\frac{1}{2} \rho V_o^2$ | overall pressure recovery coefficient  |
| 13             | fan settings                         | $l_s$         | $V_o$                                   | shroud effect on $V_o$                 |
| 14             | $l_s$                                | $x$           | $(p - p_o); \frac{1}{2} \rho V_o^2$     | reattachment point                     |
| 15             | --Data from figures 14 and 7, 8, 9-- |               |   |  |

#### IV. RESULTS AND DISCUSSION

##### Reattachment Pressure Distribution

Figures 7, 8 and 9 show the pressure distribution on the downstream surface of the shroud. In these figures the distance  $x$  measured along the shroud is normalized by the step heights,  $h$ , and the pressure is normalized as the pressure coefficient

$$C_p = \frac{p - p_o}{\frac{1}{2} \rho V_o^2}$$

where  $p_o$  and  $V_o$  are the main flow conditions upstream of the step.

The pressure distributions shown are all for the same step height but for several different shroud lengths at three different Reynolds numbers. Figure 7 is for a main stream velocity,  $V_o = 24.8$  ft/sec, figure 8 is for  $V_o = 54.8$  ft/sec and figure 9 for  $V_o = 83.4$  ft/sec. In all three cases similar features may be inferred. Immediately downstream of the step is a region of shear layer mixing of the central stream with the air in the cavity at essentially constant pressure. The next region is the reattachment region accompanied by a rising pressure. Finally redevelopment of the wall boundary layer takes place at nearly constant pressure. In these figures it can be seen that for all cases, including those for which the shroud lengths are too short for reattachment to occur, the pressure distributions are similar in that a region of constant pressure just downstream of the step is joined to the region of constant pressure downstream of the shroud by a smooth pressure rise. For the

shorter shroud length of approximately 4 step heights the pressure rise is rather abrupt in the plane of the shroud exit. This shows that the shroud is too short for proper pressure recovery inside the shroud since not enough mass has been fed into the reverse flow field from the shear layer. As a result a flow into the shroud is induced which supplies the necessary mass flow from outside the shroud and accounts for the low pressure at the lip of the shroud.

A reduced pressure coefficient based on the conditions along the nearly constant pressure portion of the shear layer just downstream of separation can be defined. In terms of the normal pressure coefficient it would be

$$\tilde{C}_p = \frac{C_p - C_{p1}}{1 - C_{p1}}$$

In the case of Roshko and Lau (Ref. 11) it was found that the overall pressure rise tended to correlate using this coefficient, but in the present investigation no such correlation was found. However, correlation is observed in the initial portion of the pressure rise region, indicating a smooth transition as the jet is more fully confined. Lack of correlation in the overall pressure rise implies that in the partially confined jet full pressure recovery to that expected for an abrupt channel expansion is incomplete.

### Radial Pressure Distribution

Figure 10 shows the radial pressure distribution for a shroud length of 10.4 inches. In the figure, pressure distributions are shown for six different downstream stations. The radial distance  $r$  is measured normal to the main flow and outward from the centerline of the jet. It is normalized by the step height,  $h$ . The normal static pressure coefficient  $C_p$  is used.

$$C_p = \frac{P - P_o}{\frac{1}{2} \rho V_o^2}$$

For radial traverses inside the shroud there is a pronounced gradient through the shear layer. This indicates appreciable streamline curvature in the shear layer. Traverses for downstream distances greater than the shroud length show a flatter profile indicating less curvature of the streamlines as shown in figure 11.

### Mean Velocity

Figure 11 shows the streamwise component of mean velocity in the mixing region for a step height of one inch and a main flow velocity,  $V_o$ , of 54.8 ft/sec. No velocity measurements were made in the reverse flow region of the recirculation bubble and this portion of the profile is represented in the figure by a dotted line. From the distribution of mean longitudinal velocity and the initial mass flow of the jet the dividing streamline was calculated. The dividing streamline starts at the step shoulder and bends towards the downstream reattachment point of the shroud. The dividing streamline can be considered as the line which divides the recirculation flow region from the main

flow of the jet. The streamline pattern of the flow also calculated from a mass balance is plotted in figure 11 as well.

### Shroud Length Effects

As longer shroud lengths are placed on the jet several effects are observable both on the parameters at the entrance of the abrupt channel expansion ( $p_o$ ,  $V_o$ ) and on the reattachment parameters ( $x_r$ ,  $\sigma_r$ ).

Figure 12 shows the effect of changing shroud length on the static pressure at the jet nozzle. An overall pressure recovery coefficient can be defined as

$$\overline{C}_p = \frac{p_a - p_o}{\frac{1}{2} \rho V_o^2}$$

where  $p_a$  is the ambient pressure into which the jet discharges,  $p_o$  is the main flow static pressure upstream of the step, and  $\frac{1}{2} \rho V_o^2$  is the actual dynamic pressure of the main flow upstream of the step. Data are presented for several initial flow velocities.  $V_o$  changes with shroud length (Fig. 13), for constant fan settings; the values of  $V_o$  listed are those with no shroud over the jet.

For shroud lengths less than two step heights the pressure recovery coefficients are very small. Beyond that point as the shroud length is increased a smooth increase is observed in the pressure recovery coefficients. For shroud lengths longer than fifteen step heights the curves appear to be approaching asymptotic values.

The continuity and momentum equations for an abrupt channel

expansion can be reduced, neglecting wall friction, to

$$\frac{p_a - p_o}{\frac{1}{2} \rho V_o^2} = 2\alpha(1 - \alpha) = \bar{C}_p$$

where  $\alpha$  is the area ratio of the channel expansion. For the present study  $\alpha$  was constant at 0.56, therefore the pressure recovery coefficient based on this is equal to 0.49. As can be seen in figure 12 the asymptotic values of  $\bar{C}_p$  fall slightly below this calculated value.

Figure 13 shows that for a constant fan setting a longer shroud length results in a higher main flow velocity at the entrance of the abrupt channel. This is simply a reflection of the fan characteristic that an increase in the pressure at the nozzle causes a decrease in the pressure difference across the fan and allows a larger mass flow to be generated by the fan.

Figure 14 shows the dependence of reattachment length,  $x_r$ , upon shroud length,  $l_s$ . Both reattachment length and shroud length are normalized by the step height,  $h$ . Data for three different Reynolds numbers are presented. For short shroud lengths the separated flow does not reattach inside the shroud. There is a minimum shroud length necessary for reattachment to be achieved which decreases as the Reynolds number increases. After this minimum has been reached as the shroud length is increased the reattachment length increases correspondingly. At a certain shroud length a maximum reattachment length is reached. This shroud length for which a maximum reattachment length is reached decreases as Reynolds number increases. The maximum reattachment length also

decreases for increasing Reynolds number.

Roschke and Back (Ref. 6) investigated reattachment downstream of an abrupt circular channel expansion for various Reynolds numbers based on the diameter of the channel upstream of the step. They found that near Reynolds number of 4,200 the reattachment length appeared to be reaching a constant value in the turbulent regime of 8-11 step heights. In this case step height to upstream diameter ratio was 4/5.

Mueller, Korst and Chow (Ref. 12) investigated this same problem with a two dimensional turbulent jet and found reattachment length to be approximately 7 step heights. Seban (Ref. 13) used flow over a two dimensional step in the turbulent regime and found reattachment to be at 5-6 step heights. In the present investigation the maximum reattachment lengths were 8 step heights for the largest Reynolds number and 10 step heights for the lowest Reynolds number.

Crabtree (Ref. 14) and Moore (Refs. 2, 3) developed a significant parameter,  $\sigma$ , the pressure recovery coefficient. An alternate parameter is

$$\sigma_r = \frac{C_{P_r} - C_{P_1}}{1 - C_{P_1}}$$

which would then be the pressure recovery factor at the point of reattachment.  $C_{P_r}$  is the normal pressure coefficient at the reattachment point and  $C_{P_1}$  is the normal pressure coefficient just downstream of separation. This coefficient,  $\sigma_r$ , has meaning only for

shroud lengths long enough for reattachment to be achieved. This reattachment pressure recovery coefficient is plotted in figure 15 for increasing shroud lengths which are normalized by the step heights,  $h$ . If  $\sigma_r$  is above some critical value of  $\sigma$ , reattachment occurs. For long shroud lengths a maximum reattachment recovery coefficient is reached. This maximum  $\sigma_r$  is approximately 0.34 and is the same for all three Reynolds numbers. The maximum reattachment length occurs when the pressure recovery coefficient reaches the value 0.34.

Kuethe (Ref. 15) analyzed the problem of predicting a reasonable value of  $\sigma$  by considering the rate of spreading of the turbulent mixing region. His results yielded a value of 0.32. The analysis of pressure distributions obtained by Dimmock (Ref. 16) in tests on a flapped airfoil found well defined separation bubbles for which  $\sigma$  was fairly constant at 0.35. Tani experimentally investigated the two dimensional case of flow over a downstream facing step. He found values of reattachment pressure coefficient from 0.20 to 0.36. The lower values were for cases in which the boundary layer at separation was large compared to the step height.

Other comparisons are shown in table 1.

| <u>Author</u>                  | <u><math>\sigma</math></u> |
|--------------------------------|----------------------------|
| Tani (Ref. 4)                  | 0.20 to 0.37               |
| Moore (Ref. 2)                 | 0.33                       |
| Seban (Ref. 13)                | 0.33                       |
| Mueller, Korst, Chow (Ref. 12) | 0.36                       |
| Roshko (Ref. 17)               | 0.34                       |

Table 1. Reattachment Pressure Recovery Coefficient



## IV. CONCLUSIONS

In this study of a partially confined jet, a shroud having a diameter of  $4/3$  the jet diameter<sup>(\*)</sup> and variable length was used to achieve various degrees of confinement. It was found that fully *confined conditions* were reached at a shroud length of about 16 step heights. For shorter shrouds the pressure distribution, while not affected in the initial portion, did not recover to the same maximum values as for full confinement.

For shroud lengths shorter than 8-10 step heights, depending on Reynolds number, reattachment onto the shroud did not occur. Nevertheless a rising longitudinal pressure distribution was still induced; the maximum pressures attained decreased with shroud length.

Shrouds of length less than about 3 step heights produced very little perturbation.

\* (thus a step height of  $1/6$  diameter)

## REFERENCES

1. Chang, P. K. : Separation of Flow. Pergamon Press, 1970.
2. Moore, T. W. F. : Some Experiments on the Reattachment of a Rearward Facing Step on a Flat Plate Aerofoil. Jour. Roy. Aero. Soc., Vol. 64 (1960), pp. 668-672.
3. Moore, T. W. F. : A Note on the Causes of Thin Aerofoil. Jour. Roy. Aero. Soc., Vol. 63 (1959), pp. 724-730.
4. Tani, I. : Experimental Investigation of Flow Separation Over a Step. Paper presented at IUTAM Symposium on Boundary Layer Research, Freiburg, Germany (1957).
5. Chaturvedi, M. C. : Flow Characteristics of Axisymmetric Expansions. ASCE Proceedings, Hydraulic Div. Jour., Issue HY-3, Vol. 98 (1963), pp. 61-92.
6. Back, L. H., Roschke, E. J. : Shear Layer Flow Regimes and Wave Instabilities and Reattachment Lengths Downstream of an Abrupt Circular Channel Expansion. Jour. of Applied Mech., Vol. 39 (1972), pp. 677-681.
7. Seban, R. A., Emery, A., Levy, A. : Heat Transfer to Separated and Reattached Subsonic Turbulent Flows Obtained Downstream of a Surface Step. Jour. Aero. Sci., Vol. 26 (1959), No. 12, pp. 809-814.
8. Macagno, E. O., Hung, T. K. : Computational and Experimental Study of a Captive and Annular Eddy. Jour. of Fluid Mech., Vol. 28, Part 1 (1967), pp. 43-64.
9. Owen, P. R., Klanfer, L. : On the Laminar Boundary Layer Separation from the Leading Edge of a Thin Aerofoil. ARC Current Paper No. 220.
10. Norbury, J. F., Crabtree, L. F. : A Simplified Model of the Incompressible Flow Past Two Dimensional Aerofoils with Long Bubble Type of Flow Separation. RAE Technical Note No. Aero 2352 (1955).
11. Roshko, A., Lau, J. C. : Some Observations on Transition and Reattachment of a Free Shear Layer in Incompressible Flow. Proceedings of the 1965 Heat Transfer and Fluid Mech. Institute, Stanford University Press (1965).
12. Mueller, T. J., Korst, H. H., Chow, W. L. : On the Separation, Reattachment, and Redevelopment of Incompressible Turbulent Shear Flow. Trans. ASME, Paper No. 63-AHGT-5.

## REFERENCES (cont.)

13. Seban, R. A. : The Effect of Suction and Injection on the Heat Transfer and Flow in a Turbulent Separated Airflow. Jour. of Heat Transfer, Trans. ASME, Series C, Vol. 88 (1966), pp. 276-284.
14. Crabtree, L. F. : Effects of Leading Edge Separation of Thin Wings in Two Dimensional Incompressible Flow. Jour. of Aeronautical Sciences, Vol. 24 (1957), pp. 597.
15. Kuethe, A. M. : Investigations of the Turbulent Mixing Regions Formed by Jets. Jour. of Applied Mech. , Vol. 2 (1935), pp. 87-95.
16. Dimmock, N. A. : Some Further Jet Flap Experiments, NGTE Memo No. M255 (1956).
17. Roshko, A. : On the Drag and Shedding Frequency of Two-Dimensional Bluff Bodies. NACA TN 3169 (1954).

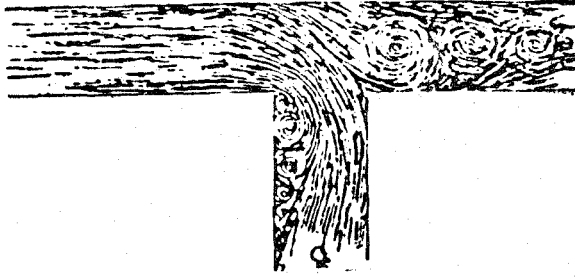


Figure 1. Sketch by Leonardo da Vinci (1452-1519). Separation and reattachment is visible. (Copied from J. Ackeret, "Aspects of Internal Flow".)

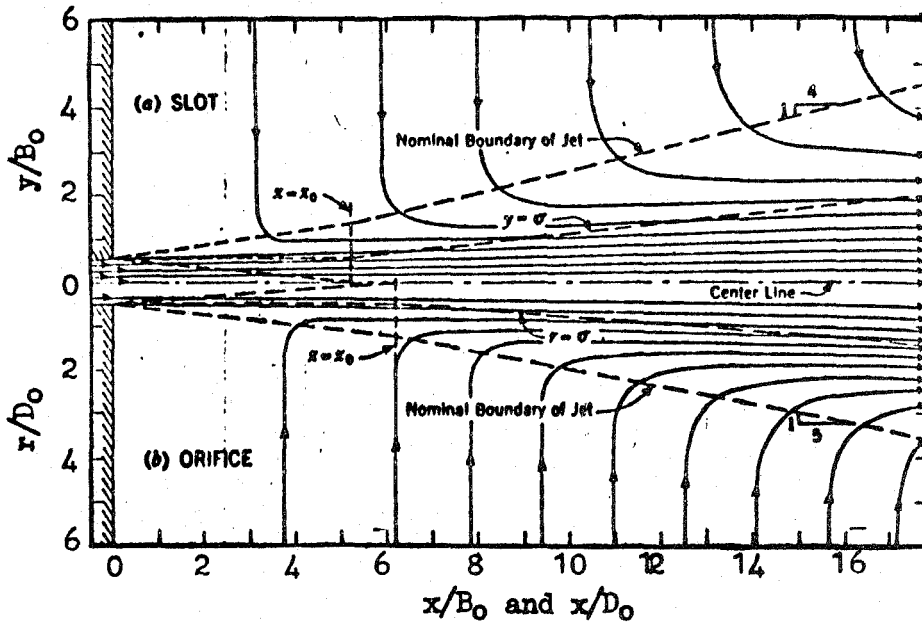


Figure 2. General Patterns of Flow from Slot and Orifice. (Copied from Albertson, Dai, Jensen, and Rouse. ASCE Trans. Vol 115.)

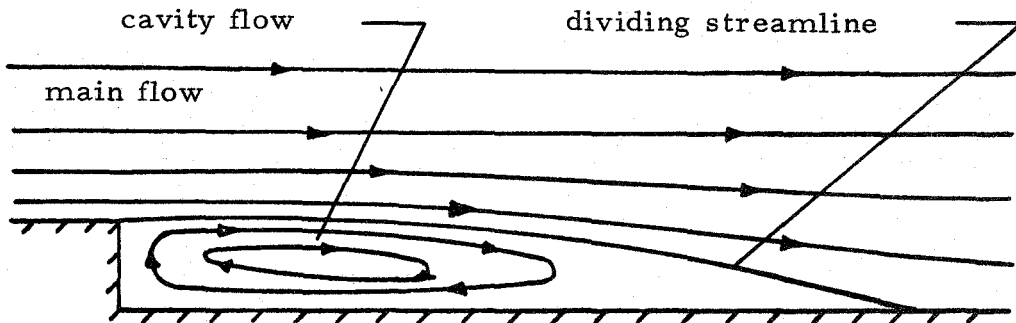


Figure 3. General Pattern of the Flow in a Confined Jet.

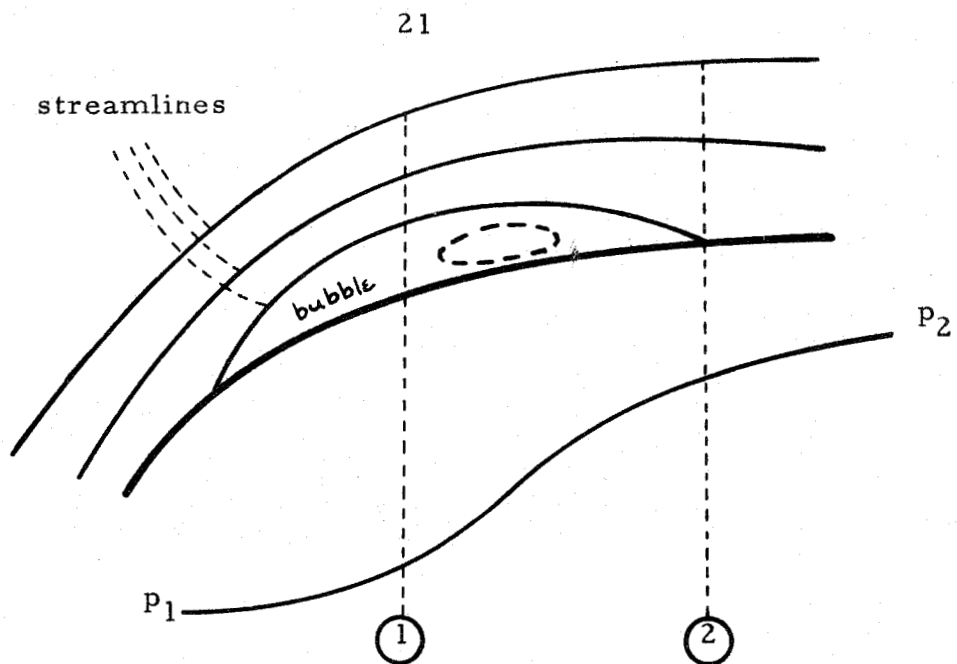


Figure 4. Separation Bubble on an Aerofoil.

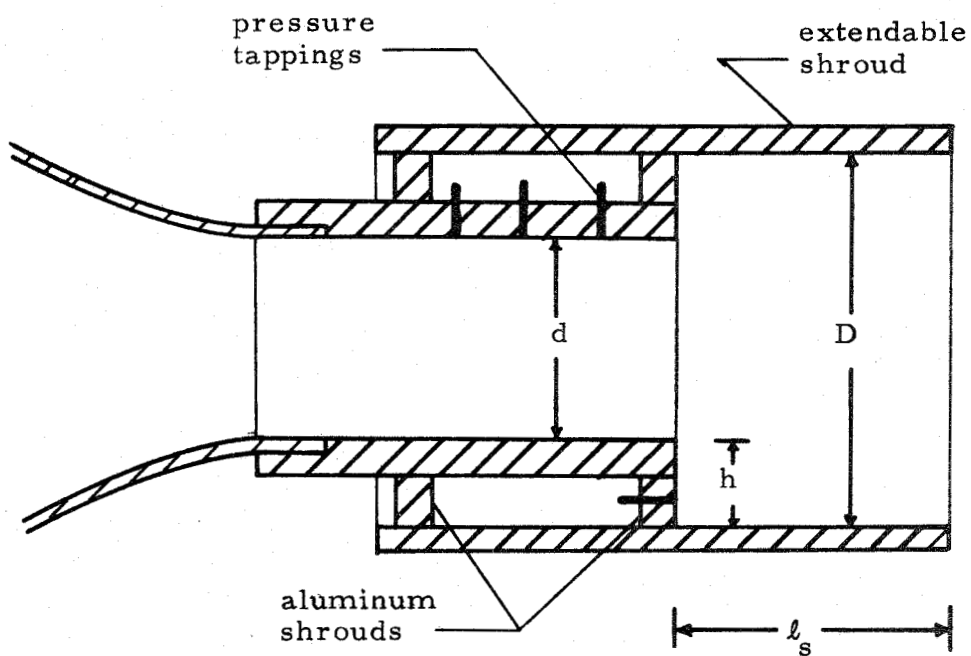
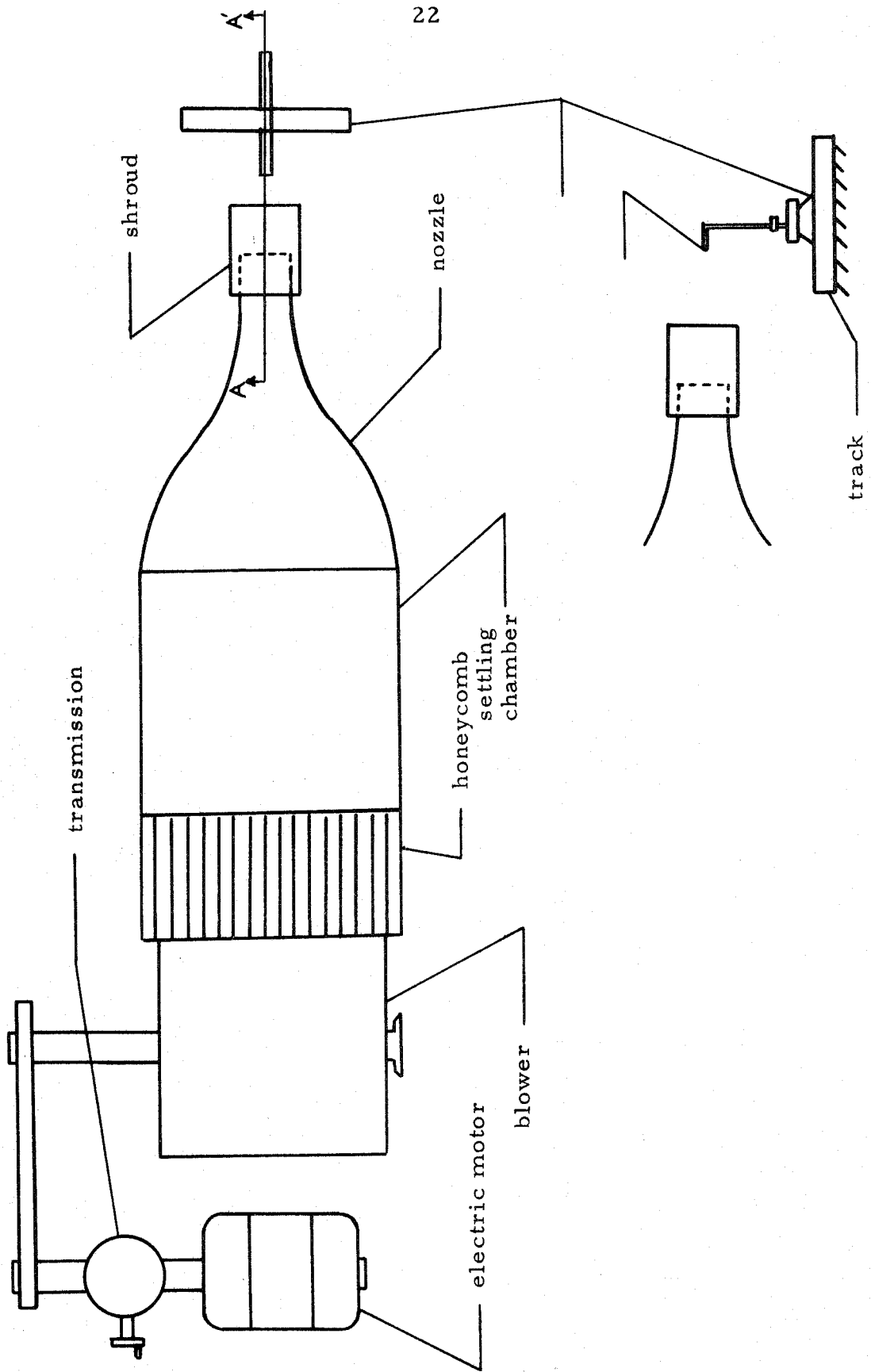


Figure 5. Test Section Configuration



Cross Section A-A'

Figure 6. Schematic of Experimental Setup.

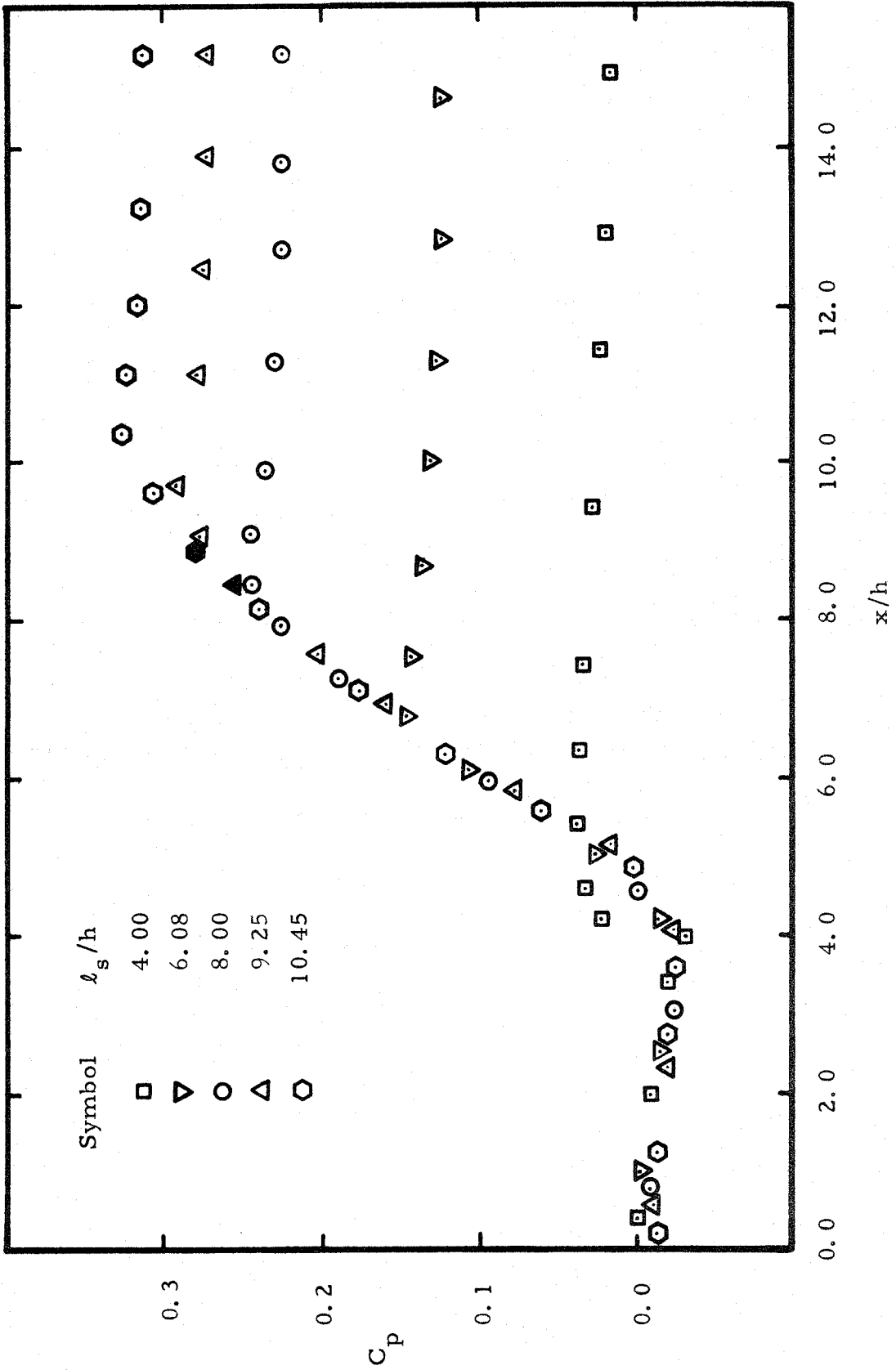


Figure 7. Reattachment Pressure Distribution. ( $V_0 = 24.8$  ft/sec)

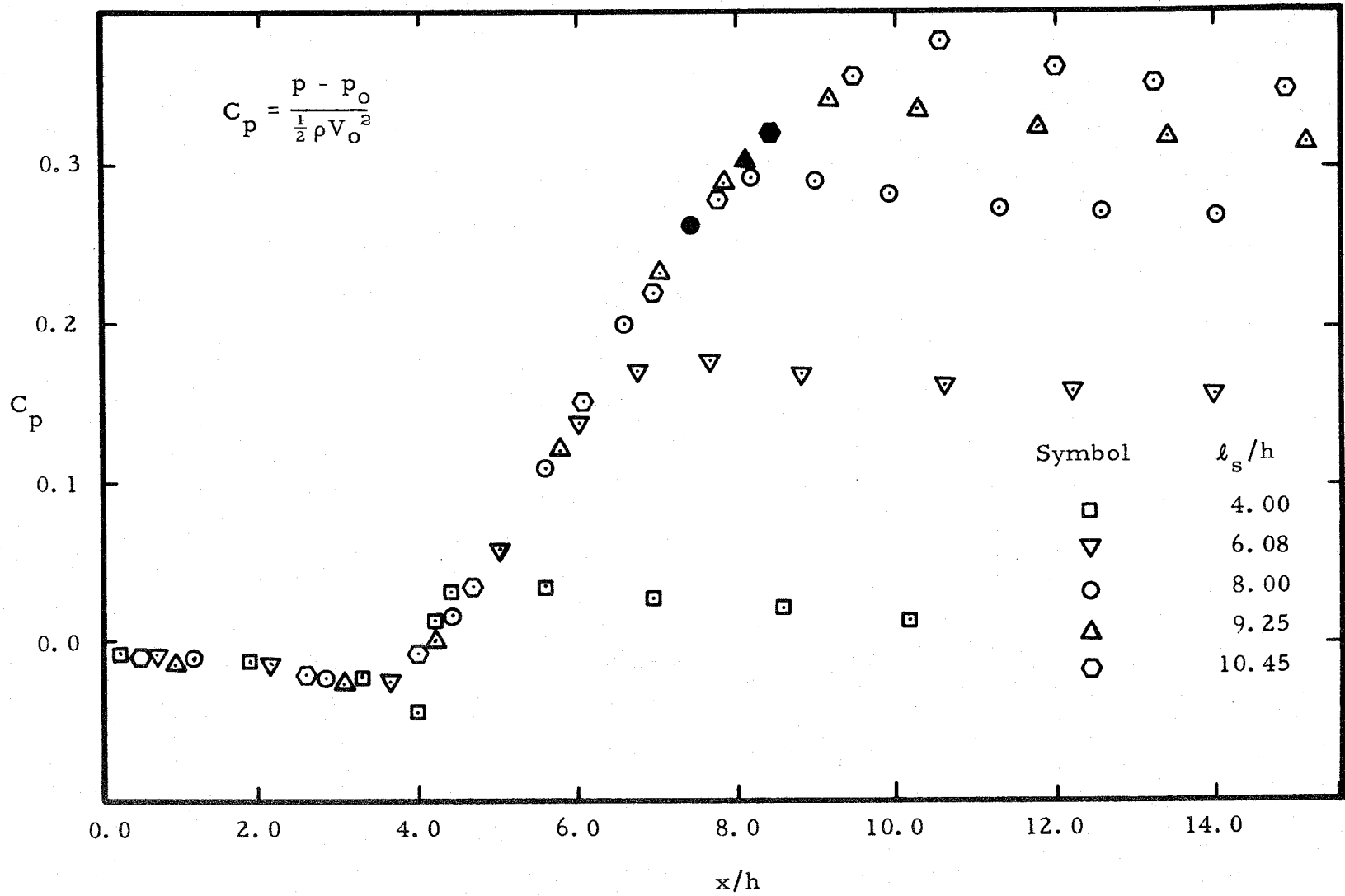


Figure 8. Reattachment Pressure Distribution. ( $V_o = 54.8$  ft/sec)



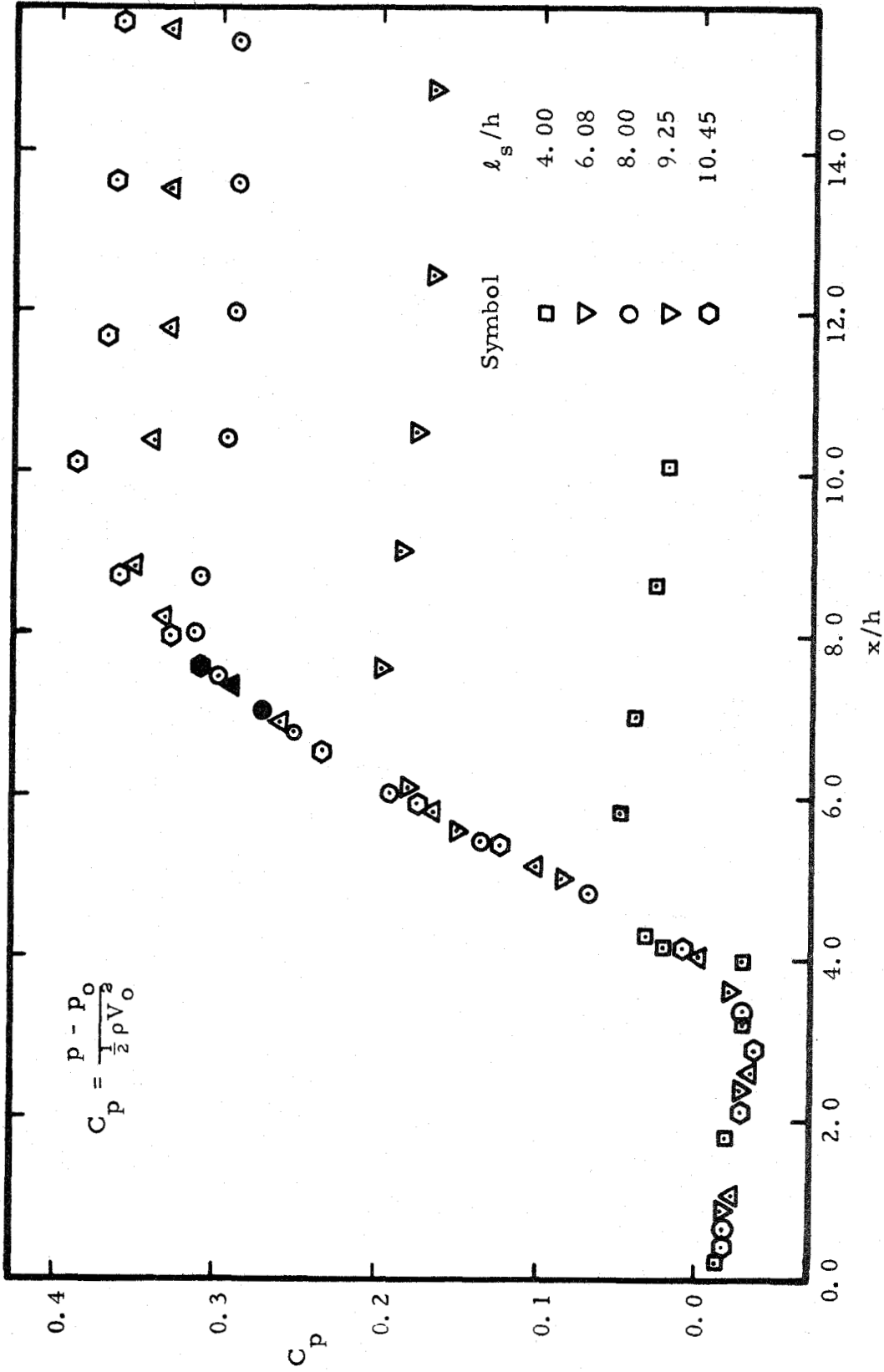
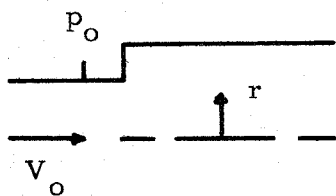


Figure 9. Reattachment Pressure Distribution. ( $V_0 = 83.4$  ft/sec)

$$C_p = \frac{p - p_o}{\frac{1}{2} \rho V_o^2}$$



| Symbol      | $x/h$ |
|-------------|-------|
| $\nabla$    | 4.0   |
| $\circ$     | 6.0   |
| $\square$   | 8.0   |
| $\odot$     | 10.0  |
| $\triangle$ | 12.0  |
| $\times$    | 14.0  |

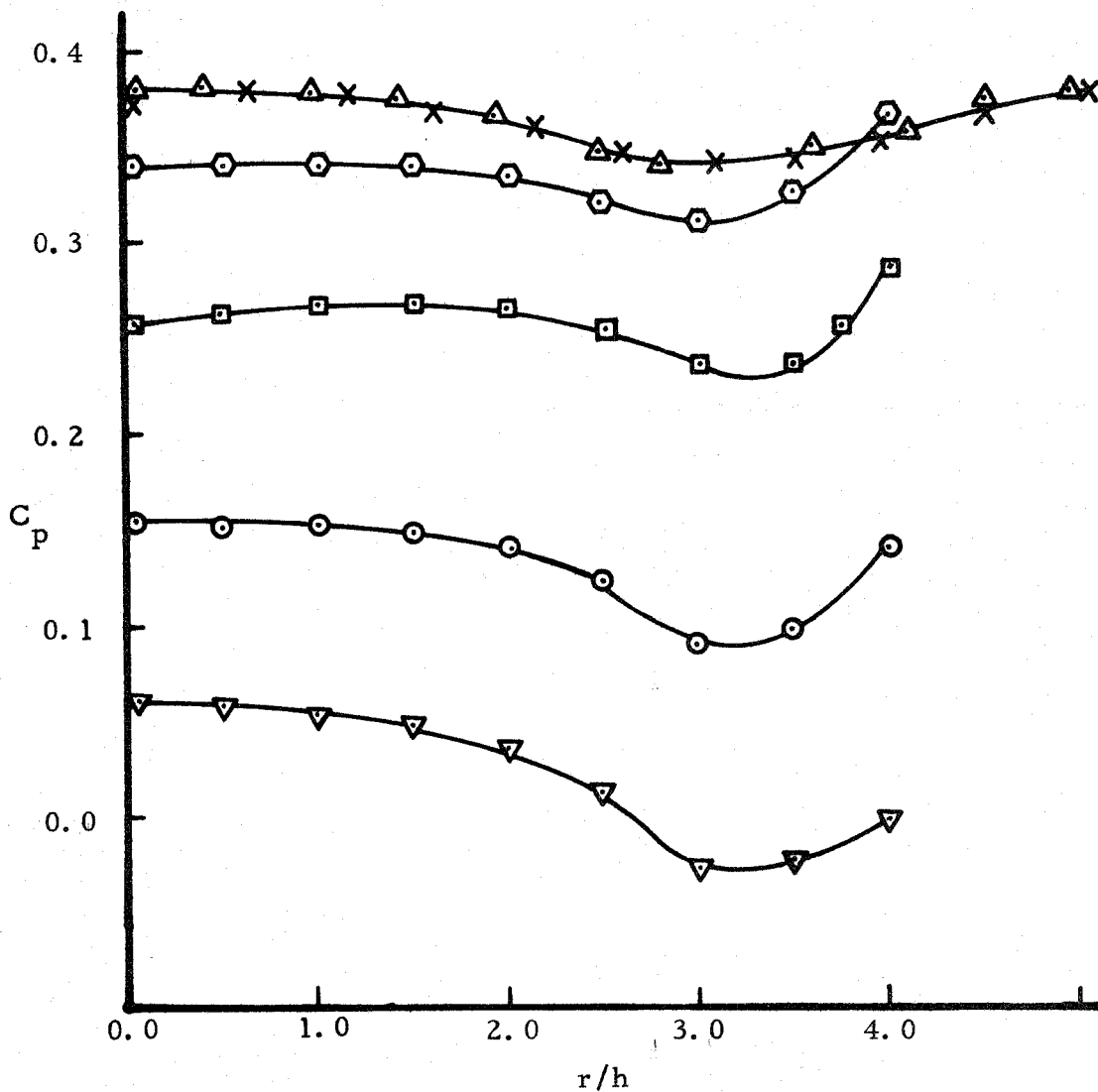


Figure 10. Radial Pressure Distribution  
( $l_s = 10.4$  inches,  $V_o = 54.8$  ft/sec)

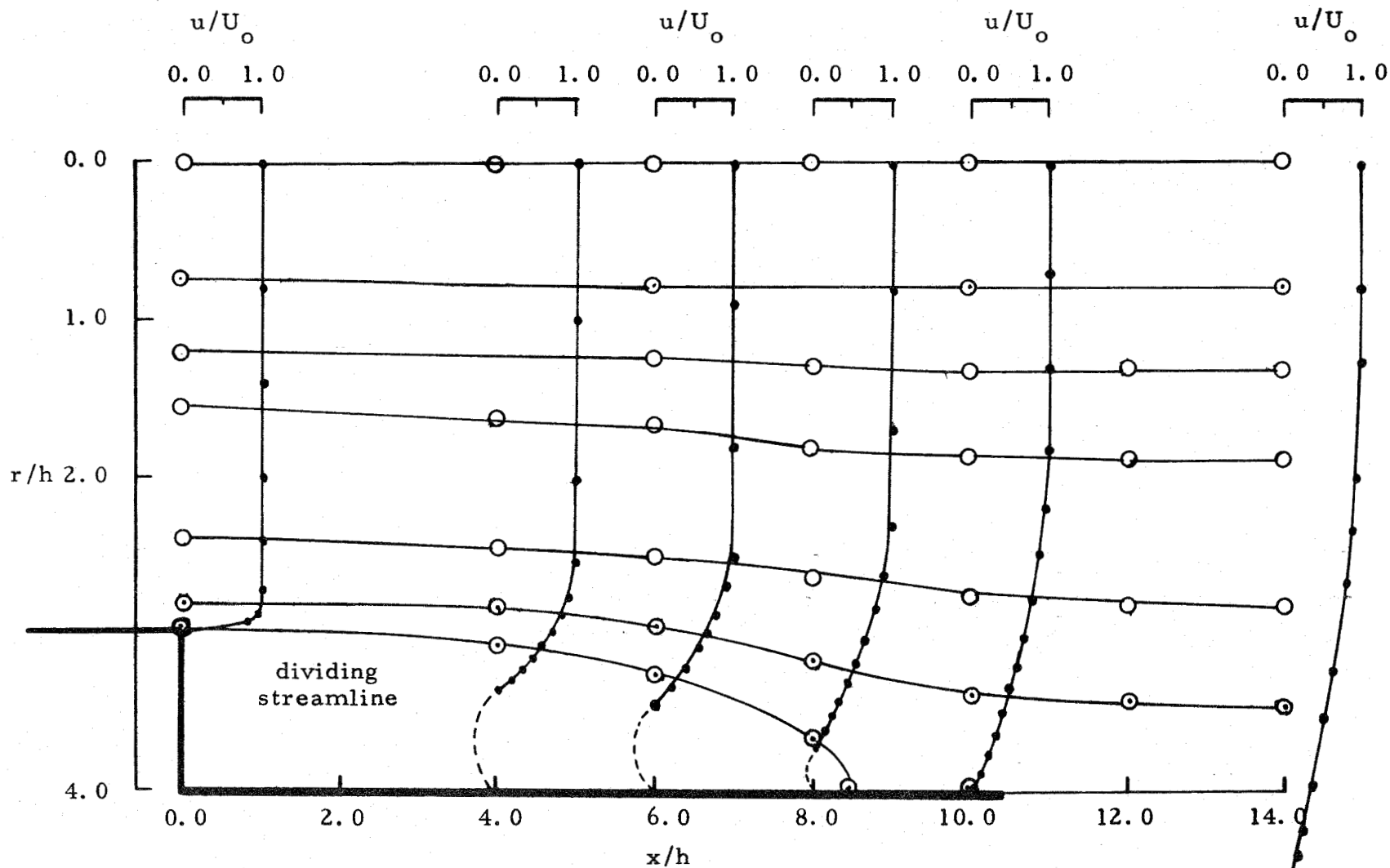


Figure 11. Mean Velocity Profiles and Streamline Patterns.  
 ( $l_s = 10.4$  inches,  $V_0 = 54.8$  ft/sec)

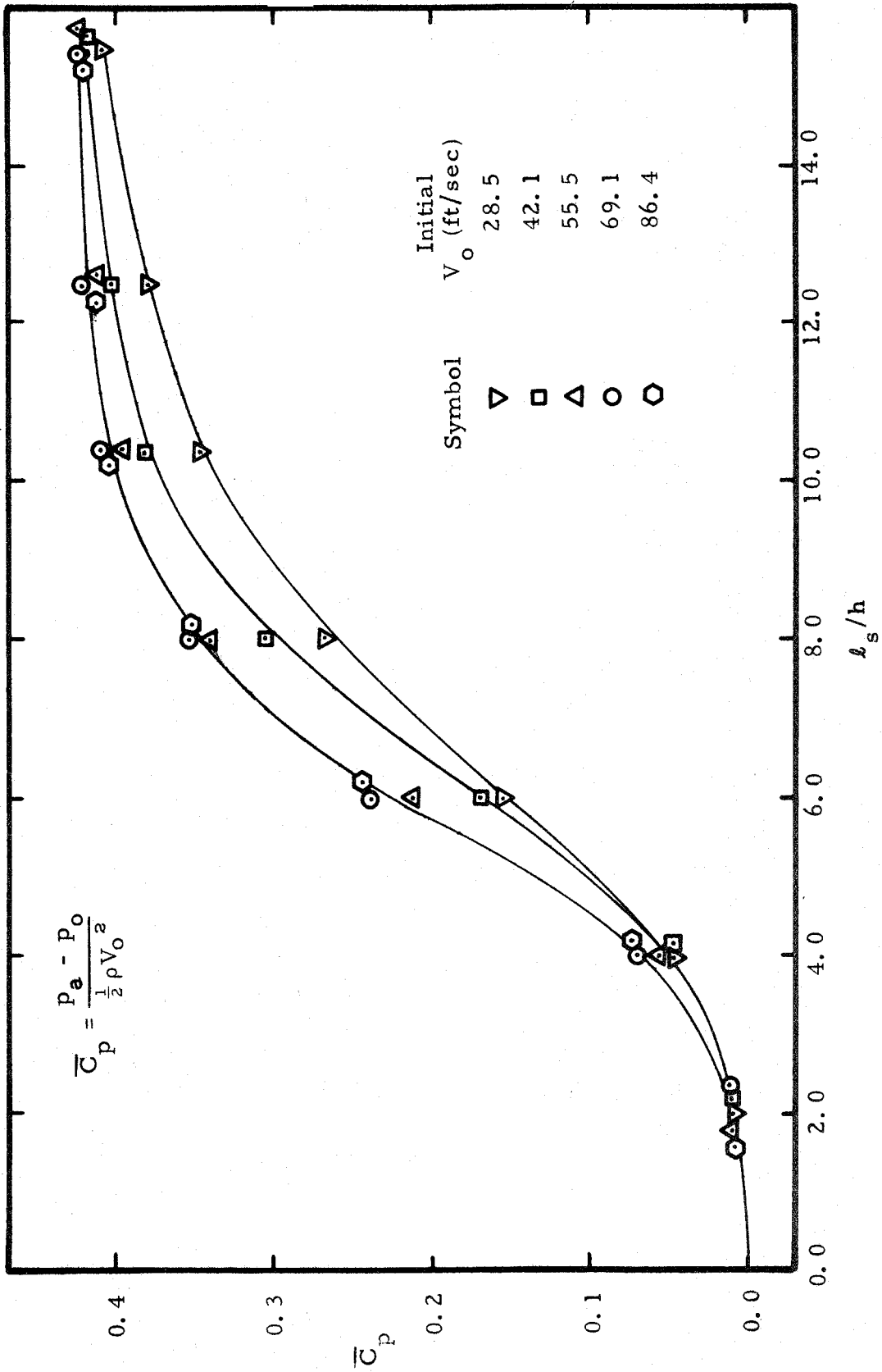


Figure 12. Overall Pressure Recovery Coefficient for Changing Shroud Lengths.

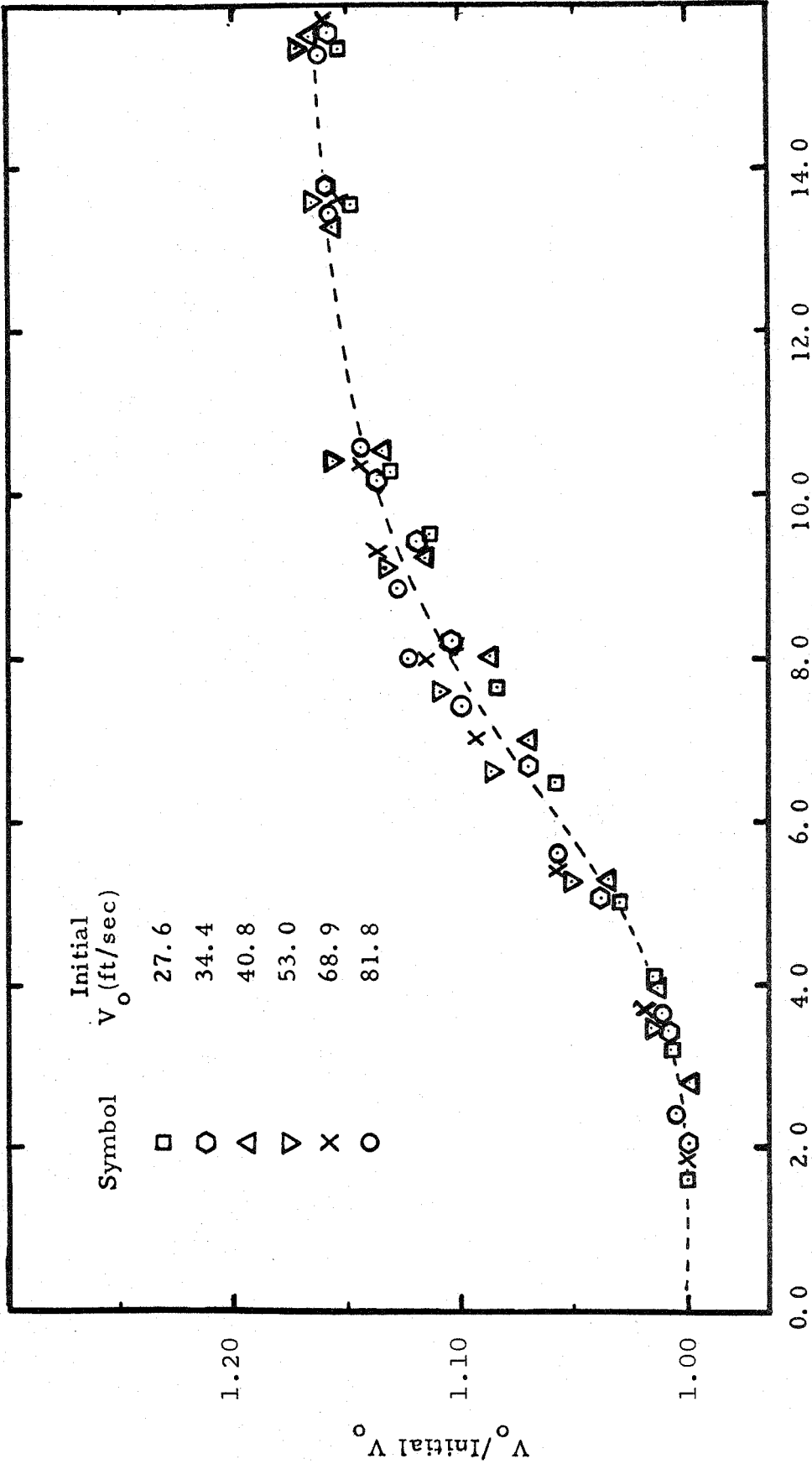
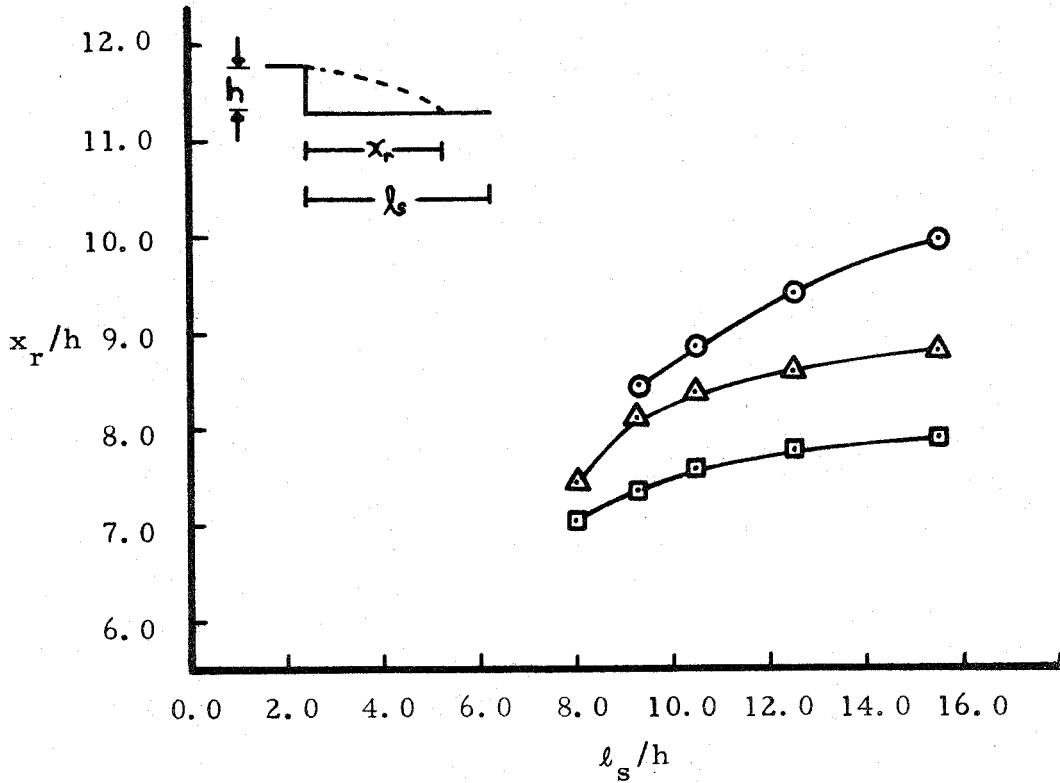
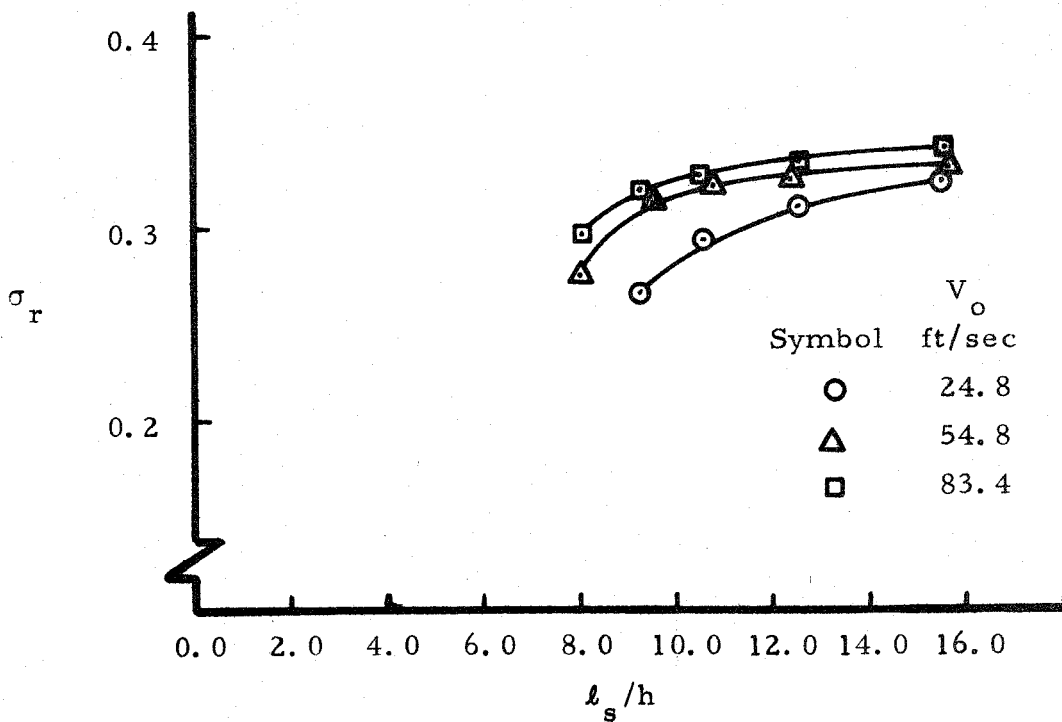


Figure 13. Change of Main Flow Velocity ( $V_0$ ) Due to Changes of Shroud Length

Figure 14. Reattachment Lengths ( $x_r$ ).Figure 15. Reattachment Pressure Recovery Coefficient ( $\sigma_r$ ).